ISSN 2176-5480

22nd International Congress of Mechanical Engineering (COBEM 2013)
November 3-7, 2013, Ribeirão Preto, SP, Brazil

VIBRATION-BASED DAMAGE IDENTIFICATION APPLIED FOR COMPOSITE PLATE: NUMERICAL ANALYSES

Murilo Sartorato
Ricardo de Medeiros
Flávio Donizeti Marques
Volnei Tita
University of São Paulo, São Carlos School of Engineering, Department of Aeronautical Engineering, Av. João Dagnone, 1100 São Carlos, SP, Brazil
medeiros@sc.usp.br, murilosart@gmail.com, fmarques@sc.usp.br, voltita@sc.usp.br

Dirk Vandepitte
Department of Mechanical Engineering, PMA – KU Leuven, Leuven, Belgium
Dirk.Vandepitte@mech.kuleuven.be

Abstract. *Maintenance planning and costs are one of the greatest logistics concerns faced today by aircraft manufactures and operators. With the advancement of composite materials, other problems arrived as these materials' behavior are still not completely understood. As such, structure health monitoring (SHM) and damage detection methods were eagerly studied in academic level in the last two decades. In particular, vibration based methods employing piezoelectric sensors and/or actuators offer a promising option, especially with the advance of piezoelectric materials such as macro-fiber composites (MFCTMs) and active fiber composites (AFC) which can be incorporated directly into the composite materials. Through these methods, damage can be estimated and located by comparing the dynamic responses between the damaged and undamaged structure. This occurs as, in general, damage locally introduces changes in the mass and stiffness properties of the structure, changing the dynamic properties of a given structure such as modal shapes, natural frequencies and damping values. In this paper, a preliminary investigation in order to develop a vibration-based damage identification method is presented, consisting on evaluating via Finite Element Method not only the mode shapes but also the Frequency Response Functions (FRFs) of undamaged and damaged composite plates. Therefore, rectangular plates made of composite material, resin epoxy and carbon fiber, were analyzed by Abaqus' code, considering piezoelectric transducers attached in suitable positions in order to obtain the dynamic behavior of the structures. A FE mathematical formulation for laminate structures containing active piezoelectric layers was developed in order to obtain more accuracy results. Thus, a plate quadratic finite element with eight nodes and curved structures, which allows fully coupled electromechanical analyses was formulated and implemented into the Abaqus' code, using Fortran subroutine defined as UEL (User Element). First, an undamaged composite plate was modeled using this user subroutine. Then natural frequencies and Frequency Response Functions were obtained by finite element analyses. After that, a central hole is created in the finite element model in order to simulate a specific damage. Then, the natural frequencies and Frequency Response Functions were obtained for the damaged plate. Finally, it was discussed the advantages and limitations to use vibration-based damage detection method into the context of SHM (Structural Health Monitoring) via Finite Element approach.*
Keywords: *Structural health monitoring, damage metrics, vibration experimental data, piezoelectric sensor, nondestructive inspection, Vibration-based method.*

1. INTRODUCTION

The aeronautical industry, due to the increasing project requirements that exist in order to guarantee airworthiness and high levels of safety lives in a paradoxical environment. From one side, it must follow rigorous safety requirements that lead to heavy structures and costly maintenance programs, and from the other side low maintenance costs and on low weigh is desirable. For that reason, several design and maintenance philosophies were created based on damage tolerance procedures and complex maintenance inspections schedules. One of the most common objectives in modern aeronautical design is to enable more operation hours of an aircraft with fewer inspections by calculating optimized inspection periods depending on the average mission and structural properties of the primary elements. However, several problems exist for these procedures, mainly logistic problems and the current understanding of damage progression in the different materials used in the industry, particularly in composite materials, being lacking. In this context, the detection of damage on composite structures has been one of the major challenges and concerns of airline operators, aircraft structural designers and researchers.

Regarding the above scenario, Structural Health Monitoring (SHM) is an acceptable practice not only for minimizing the number of inspections, but also for maximizing the numbers of suitable inspection periods, indispensable inspections that are able to check several different elements and components. Therefore, SHM can replace the traditional maintenance plan, reducing the operational costs of the airplane and preventing needless checks.

ISSN 2176-5480

However, both the creation and executing of a SHM system is still a challenge and an open problem. Vibration based SHM systems are one of the currently studied proposes to the use of such systems due to the relative ease of instrumentation and being computationally simple without any need for an updated numerical model. Most notable among these techniques are based on natural frequency, mode shape curvatures, modal flexibility and its derivatives, modal stiffness, modal strain energy, frequency response function and its curvature, and power spectral density (PSD). Important advances in this field have been described by Doebling et al. (1996); Salawu (1997); Doebling et al. (1998); Zou et al. (2000); Carden and Fanning (2004); Montalvão et al. (2006); Worden et al. (2008); Fan and Qiao (2011); Liu and Nayak (2012) which have been presented comprehensive reviews on SHM systems.

Great part of the problem with vibration based methods are the types for sensors used due to common accelerometers and piezoelectric ceramics introducing discontinuities in the geometry, causing stress concentration. Also, for composite materials, the inability to sense data from the inner layers is a problem. The development of piezoelectric materials in the form of thin fibers in the last years improved their usability for such applications, creating smart composite structures.

However, both numerical and experimental problems still exist with such approach: experimentally, the small experience and works in the literature existing with such type of sensors and the lack of metrics for the identification and localization of damage; numerically, models used for the dynamic analyses and for the types of sensors used.

Regarding numerical approaches, in general, the studies made fall into the different models of finite elements that can be used to correctly model damage and the electro-magnetic coupling of piezoelectric sensors. About the finite elements approaches, numerous works have been published in the last years about how to correct simulate the mechanical behavior of such structures and, therefore, several models already exist for the correct modeling of piezoelectric materials integrated with both isotropic and laminated materials. Some researchers like Wang and Qiao (2007) and Paik et al. (2007) defend that simpler models cannot completely simulate a smart composite, and simulations must be made using a micro-scale modeling of each fiber. These approaches come with a great computational cost and are impractical for analysis large structures as several methods and SHM metrics requires frequency based analysis, which need fast and efficient models. This inefficiency is caused by the use of solid elements, which are naturally costly computationally. As such, several researchers implement plate finite element models that simulate smart composites; in particular, some researchers like Marinkovic et al. (2007) presented linear plate finite element models for active composites with increasing complexity theories, yet few offer comparisons of the bi-dimensional models to already implemented ones.

This work presents a formulation of a quadratic bi-dimensional finite element capable of simulating composite structures manufactured using smart laminated materials, with piezoelectric layers, or composite materials with thin piezoelectric actuators attached to its surface. This formulation was implemented within Abaqus commercial finite element package using Fortran subroutines through its UEL (User Element) tool. An experiment consisting of a simple curved composite plate was made by doing modal analysis. The plate was then holed in the center for the simulation of damage. Then, the same studies were made using piezoelectric sensors over four points of the plate and simulated numerically using the proposed model. Frequency response functions were obtained and the results between the experiment, and the numerical simulations for both accelerance and the piezoelectric response were compared. Finally, conclusions were made for the use of numerical simulations with a SHM environment, the advantages in the use of piezoelectric sensors for SHM and ways to characterize damage identification.

2. FINITE ELEMENT MODEL

In this section, a summary of the theoretical model of the implemented finite element is presented. The geometric description of the shell is based on the degenerated shell element theory. The constitutive equations for a piezoelectric active layer and for a smart composite laminate were based upon the works of Damjanovic (2006), Marinkovic et al. (2007) and Deraemaeker et al. (2009). For a more detailed development of the implemented finite element, see the reference Sartorato (2012). It should be noted that for the whole formulation the indexes are in the following range: i=1..3, j=1..3, k=1..2, n=1..8.

2.1 Geometric description of the shell: coordinates, displacements and strains

Degenerated shell elements are simple or double curved bi-dimensional finite elements. These elements are geometrically described from the degeneration of a cuboid solid in a bi-dimensional surface using some surface as reference, either middle, bottom or top surfaces. For the following formulation, the middle surface is used as reference. This description can be done by the use of the shell thickness h and three distinct coordinate systems, shown in Fig. 1: the isoparametric system (ξ_1, ξ_2, ξ_3), the global system (X_1, X_2, X_3) and the local system (S_1, S_2, S_3) (Zienkiewicz e Taylor, 2000). Also in Fig. 1 are shown the coordinate transformation matrixes between each coordinate system. Using these three coordinate systems, the displacement of a given point in a shell can be written using five degrees of freedom: the three translation components of the displacement of the middle surface (u_1, u_2, u_3) and the two rotations of

ISSN 2176-5480

the shell in that point (θ_1, θ_2). The mathematical expression for the displacement can be found in Eq. 1, while the transformation matrixes H and T are shown in Eq. 2.

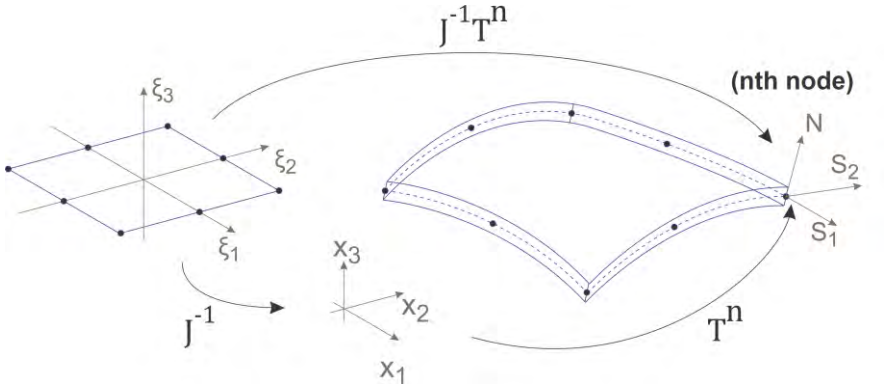

Figure 1. Coordinates systems and transformations used in the finite element formulation.

$$\bar{u} = \begin{Bmatrix} u_1 \\ u_2 \\ u_3 \end{Bmatrix} + \xi_3 \frac{h}{2} H \begin{Bmatrix} \theta_1 \\ \theta_2 \end{Bmatrix} \tag{1}$$

$$H = \begin{bmatrix} -T_2 \\ T_1 \end{bmatrix}^T, \quad T_3 = \left\| \frac{\partial X}{\partial S_1} \times \frac{\partial X}{\partial S_2} \right\|, \quad T_2 = \begin{cases} T_3 \times (1,0,0), T_3^1 < \cos(0.1°) \\ T_3 \times (0,0,1), T_3^1 > \cos(0.1°) \end{cases}, \quad T_1 = T_2 \times T_3, \quad J^{-1} = \frac{\partial \xi}{\partial X} \tag{2}$$

With the mathematical description of the displacements, the engineering strains in a given point can be calculated through their definitions from the symmetric gradient of the displacements. The expression for the strains can be found in Eq. 3. Equation 3 shows that using this theory, the resulting strains naturally recovers the First-Order Shear Theory assumptions for the strains of a plate: the strains can be separated in an independent term, equal to the strain in the middle surface and a term linearly proportional to the thickness of the shell and its curvature (bending or torsional).

$$\varepsilon_{ij} = \frac{1}{2}\left(\frac{\partial \bar{u}_i}{\partial S_j} + \frac{\partial \bar{u}_j}{\partial S_i} \right) = \frac{\partial u_i}{\partial S_j} + \xi_3 \frac{h}{2} H_{ik} \frac{\partial \theta_k}{\partial S_j} + \frac{h}{2} H_{ik} \theta_k \delta_{3j} \tag{3}$$

2.2 Smart composite constitutive equations

The constitutive equation for a lamina of a smart composite material is given by Eq. 4. This relation uses the convention that the 1 direction is given by the direction of the fiber; the 2 direction is within the plane defined by the lamina; and the 3 direction is transversal to the plane of the lamina. Also, this constitutive equation is formulated based upon the e-form of the general piezoelectric constitutive equation combined with the following hypothesis: orthotropic material, quasi-3D stress (σ_3=0) and uniaxial electrical polarization in the direction transversal to the piezoelectric fibers (E_1=E_2=0).

$$\begin{Bmatrix} \sigma_{11} \\ \sigma_{22} \\ \sigma_{12} \\ \tau_{23} \\ \tau_{13} \\ D_3 \end{Bmatrix} = \begin{bmatrix} Q_{11} & Q_{12} & 0 & 0 & 0 & -e'_{31} \\ Q_{12} & Q_{22} & 0 & 0 & 0 & -e'_{31} \\ 0 & 0 & Q_{66} & 0 & 0 & 0 \\ 0 & 0 & 0 & Q_{44} & 0 & 0 \\ 0 & 0 & 0 & 0 & Q_{55} & 0 \\ e'_{31} & e'_{31} & 0 & 0 & 0 & d'_{33} \end{bmatrix} \begin{Bmatrix} \varepsilon_{11} \\ \varepsilon_{12} \\ \varepsilon_{22} \\ \gamma_{23} \\ \gamma_{13} \\ E_3 \end{Bmatrix} \tag{4}$$

where, σ_{ij}, τ_{ij}, ε_{ij}, γ_{ij}, D_3 and E_3 are respectively: the membrane stresses, transversal stresses, membrane strains, transversal distortions, electrical displacement and electrical field; Q_{ij}, e'_{31} and d'_{33} are effective properties of a lamina under the aforesaid hypothesis, given by Eqs. 4 and 5 in term of the short-circuit elastic properties C^E_{ij}, the dieletrical properties d_{ii} and the piezoelectric coupling properties e_{ij}. It should be noted that, for the piezoelectric layers of a given

ISSN 2176-5480

smart composite, the transversal isotropic hypothesis is commonly used, as such $Q_{44}=Q_{55}$. Also, for the pure structural (non-piezoelectric) layers, the dieletrical and piezoelectric coupling properties can be approximated by zero.

The laminate constitutive equation can be obtained by the integration of mechanical stresses and electrical fields over the laminate thickness. As the result of this integration the working efforts over the laminate are obtained. Different from the Classical Laminated Theory, in addition to the normal (N) and bending (M) efforts, the degenerated shell theory, in conjunction to the aforementioned constitutive equation generates shearing (Q) and torcional moments efforts (T). Also, the introduction of the piezoelectric coupling produces the working electrical displacement over the laminate (D_e). These working efforts are given by Eqs. 5 to 9, where m is the number of layers in a given laminate.

$$N_{ij} = \sum_{o=1}^{m} \int_{h_o}^{h_{o+1}} \sigma_{ij} dS_3 \tag{5}$$

$$M_{ij} = \sum_{o=1}^{m} \int_{h_o}^{h_{o+1}} \xi_3 \sigma_{ij} dS_3 \tag{6}$$

$$Q_{ij} = \sum_{o=1}^{m} \int_{h_o}^{h_{o+1}} \frac{5}{4}\left(1 - \frac{4{S_3}^2}{h^2}\right) \tau_{ij} dS_3 \tag{7}$$

$$T_{ij} = \sum_{o=1}^{m} \int_{h_o}^{h_{o+1}} \xi_3 \frac{5}{4}\left(1 - \frac{4{S_3}^2}{h^2}\right) \tau_{ij} dS_3 \tag{8}$$

$$D_e = \sum_{o=1}^{m} \int_{h_o}^{h_{o+1}} E_3 dS_3 \tag{9}$$

Using the assumption that the membrane strains and the electrical field have a uniform distribution over the thickness of the laminate and the transversal distortions have a parabolic distribution over the thickness, the laminate constitutive equation can be written as an extended ABBD matrix obtained from the Classical Laminate Theory by incorporating the aforementioned extra working efforts and the piezoelectric coupling and dielectric effects. The full development of the mechanical part of the constitutive matrix ABBD-GH matrix can be seen in the Qatu et al. (2010) reference. The electrical part is described in Sartorato (2012). The final constitutive matrix for a smart composite is then given by Eq. 10.

$$\begin{Bmatrix} N \\ M \\ Q \\ T \\ D_e \end{Bmatrix} = \begin{bmatrix} A & B & 0 & 0 & -\bar{e}_1 \\ B & D & 0 & 0 & -\bar{e}_2 \\ 0 & 0 & G & G_h & 0 \\ 0 & 0 & G_h & H & 0 \\ \bar{e}_1 & \bar{e}_2 & 0 & 0 & \bar{d} \end{bmatrix} \begin{Bmatrix} \varepsilon \\ \kappa \\ \gamma_0 + \gamma_1 \\ \gamma_t \\ E_3 \end{Bmatrix} \tag{10}$$

Moreover, by the assumption that the electrical field is uniform over the thickness of the laminate, it can be written as a function of the difference of potential between the two surfaces of a given lamina (φ), as shown by Eq. 11. Also, it should be noted that, as the hypothesis that the piezoelectric layers are polarized only in the 3 direction, the lamina orientation does not influence the piezoelectric coupling and dielectric matrixes, as such, there is no need to apply the coordinate transformation matrix from the local lamina system to the laminate global system to the piezoelectric and dielectric terms.

$$E_3 = -\frac{1}{h_m}\varphi_m \tag{11}$$

2.3 Finite element formulation

Discretizing the six degrees of freedom given by the geometry and electric description of a smart composite shell, using the quadratic Lagrange serendipity shape functions ϕ_n, such as each element as 8 nodes, both the strains and electrical field can be written as function of the nodal degrees of freedom using several matrixes, following Eq. 12 and Eq. 13, where $\tilde{u}=u^n_i$ and $\tilde{\varphi}=\varphi^n_i$. The explicit mathematical description of the B matrixes can be found in the work of Sartorato (2012).

ISSN 2176-5480

$$X_i = X_i^n \Phi_n\,,\ u_i = u_i^n \Phi_n\,,\ \theta_k = \theta_k^n \Phi_n\,,\ \varphi = \varphi^n \Phi_n \tag{12}$$

$$\begin{Bmatrix} \varepsilon_{11} \\ \varepsilon_{12} \\ \varepsilon_{22} \\ \gamma_{23} \\ \gamma_{13} \end{Bmatrix} = \begin{pmatrix} B_{m_0}^u + B_{m_0}^\theta + \xi_3 B_{m_1}^\theta \\ B_{t_0}^u + B_{t_0}^\theta + \xi_3 B_{t_1}^\theta \end{pmatrix} \tilde{u}\,,\quad E_3 = B_\varphi \tilde{\varphi} \tag{13}$$

The variational equilibrium equation of a single element is found in Eq. 14, where U is the volume integration over the element of the specific electric-mechanical enthalpy (or Gibbs' piezoelectric energy), K is the kinematic energy, and P is the work from the external loads. This relation can be expanded in the element equilibrium equation, found in Eq. 15.

$$\delta\Pi = \delta U + \delta K + \delta P = 0 \tag{14}$$

$$\begin{aligned} \int_\Omega \rho(\delta\tilde{u}\cdot\tilde{u} + \xi_3\delta\theta\cdot\tilde{u} + \xi_3\delta\tilde{u}\cdot\theta + {\xi_3}^2\delta\theta\cdot\theta) + \delta\varepsilon : C^E\varepsilon - \delta\varepsilon : e'^T E_3 - \delta E_3 : e'\varepsilon - \delta E_3 d' E.d\Omega = \\ \int_\Omega \delta u\cdot b.d\Omega + \oint_\Gamma \delta u\cdot t.d\Gamma + \delta u\cdot F + \delta\theta\cdot M - \oint_\Gamma \delta\varphi\cdot q - \delta\varphi\cdot Q \end{aligned} \tag{15}$$

where ρ is the density of the plate; b, t, q, F, and Q are, respectively, the body forces, surface forces, electrical charges distribution over the surface of an electrode, concentrated forces and electrical charges. Using the simplification matrixes in Eq. 16, the final system of equations for the piezoelectric problem can be given by Eq. 17, and its terms are calculated using Eqs. 18 to 24, where w_i and w_j are Gauss' Quadrature weights.

$$B_u^m = \begin{bmatrix} B_{m_0}^u + B_{m_0}^\theta \\ B_{m1}^\theta \end{bmatrix},\ B_u^t = \begin{bmatrix} B_{t_0}^u + B_{t_0}^\theta \\ B_{t1}^\theta \end{bmatrix},\ B_{u\varphi} = \begin{bmatrix} B_{m_0}^u \\ B_{m1}^\theta \end{bmatrix},\ H0_{i,5(n+1)+j} = \delta_{ij}\Phi_n\,,\ H1_{i,5(n+1)+j} = \delta_{(i,j+3)}\frac{h}{2}\Phi_n H_{ij}^n \tag{16}$$

$$\begin{aligned} M\ddot{u} + K_{uu}u + K_{u\varphi}\varphi &= F \\ K_{\varphi u}u + K_{\varphi\varphi}\varphi &= Q \end{aligned} \tag{17}$$

$$M = \sum_{i,j=1}^{2} \det\left(J^{-1}\right) w_i w_j \rho\left[\frac{h}{2}H_0^T H_0 + \frac{h^2}{4}\left(H_1^T H_0 + H_0^T H_1\right) + \frac{h^3}{12}H_1^T H_1\right] \tag{18}$$

$$K_{uu} = \sum_{i,j=1}^{2} \det\left(J^{-1}\right) w_i w_j \left(B_u^{m\,T}\begin{bmatrix} A & B \\ B & D \end{bmatrix} B_u^m\right) + \sum_{i,j=1}^{1} \det\left(J^{-1}\right) w_i w_j \left(B_u^{t\,T}\begin{bmatrix} G & G_h \\ G_h & H \end{bmatrix} B_u^t\right) \tag{19}$$

$$K_{\varphi u} = \sum_{i,j=1}^{2} \det\left(J^{-1}\right) w_i w_j B_{u\varphi}^{\ T}\begin{bmatrix} \bar{e}_1 \\ \bar{e}_2 \end{bmatrix} B_\varphi \tag{20}$$

$$K_{u\varphi} = \sum_{i,j=1}^{2} \det\left(J^{-1}\right) w_i w_j B_\varphi^{\ T}\begin{bmatrix} \bar{e}_1 & \bar{e}_2 \end{bmatrix} B_{u\varphi} \tag{21}$$

$$K_{u\varphi} = \sum_{i,j=1}^{2} \det\left(J^{-1}\right) w_i w_j B_\varphi^{\ T}\bar{d} B_\varphi \tag{22}$$

$$F = \int_\Omega (H_0^{\ T} + \xi_3 H_1^{\ T}) b d\Omega + \oint_\Gamma (H_0^{\ T} + \xi_3 H_1^{\ T}) t d\Gamma + \Phi_n F_i^k \tag{23}$$

$$Q = -\oint_\Gamma \frac{1}{h_n} q_n d\Gamma - B_\varphi^{\ T}\cdot Q \tag{24}$$

ISSN 2176-5480

3. EXPERIMENTAL AND FINITE ELEMENT ANALAYSIS

Both the experimental and numerical analysis were based upon the modal investigation of a curved composite plate with a $[0°]_8$ lay-up configuration, uniform plies with equal thickness. The composite plate properties were given by Ribeiro et al. (2012), similar to Tita et al. (2008). The plate geometry consists of a length 305 mm, width of 244 mm and total thickness of 2.16 mm and a small curvature. For the simulation of damage, an hole with an approximate diameter of 8 mm was drilled in the center of the plate.

3.1 Experimental setup

The experimental analyses were carried out with vibrations tests in the composite plate using the coupon shown in Fig. 2. Accelerometers (PCB Piezotronix) were attached to one of its faces in the two points indicated in Fig. 2a. The input used was a pulse signal to produce the excitation on the structure originated form an impact hammer (PCB Piezotronix). Sixty three points of impact were carried out in the white circles shown in Fig. 2. The plate was then holed in its center to simulate damage.

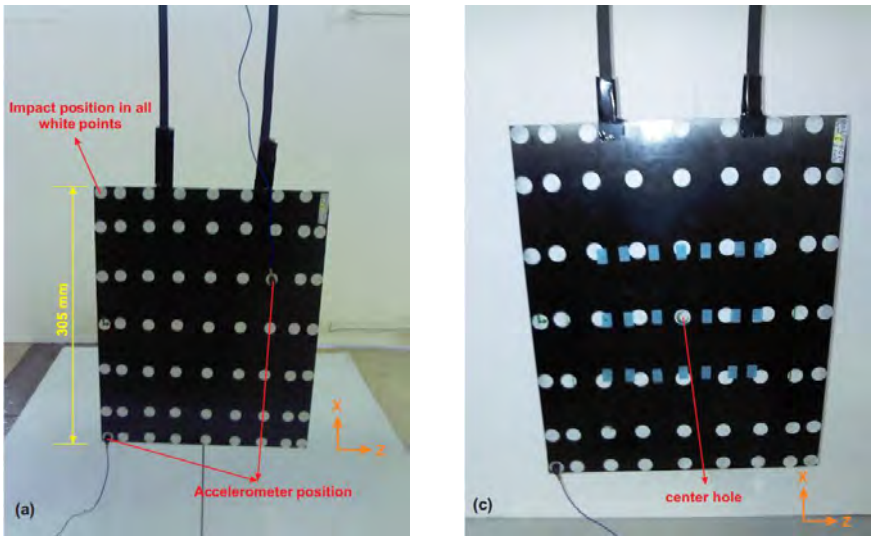

a b

Figure 2. Experimental model: a) Intact; b) damaged by drilling a center hole.

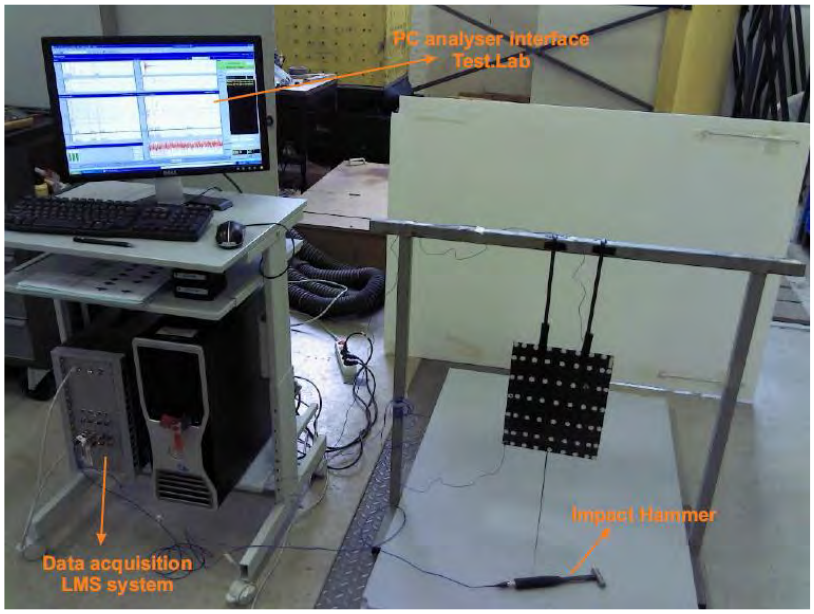

Figure 3. General layout of the experiment and the equipment used

ISSN 2176-5480

The experimental analyses consist of verifying dynamically the response of the plate. The data acquisition set-up used in the experimentation was controlled by a Test.Lab (signal acquisition LMS Test.Lab), which is a plug and play, multifunction analog, digital and timing I/O board for USB bus computers. The experimental setup for the vibration test consists of specimens to be tested, schematically show both damaged and intact in Fig. 3, accelerometers, impact position, an impulse hammer, wire connections, a personal computer equipped with data acquisition software and a PC analyzer interface. Both damaged and undamaged structures were assessed by acquiring the FRF signatures for every the accelerometers for all impacted positions. Each time signal gathered consisted of 2048 points and were sampled at 1024 Hz. The FRFs were calculated from both the measured force and response signals (accelerometers). The number of averaging individual time records was selected to be eight in order to reduce the random fluctuation in the estimation of the FRFs. The free-free conditions were simulated suspending the beam with springs introducing an extra natural frequency, reasonably lower than the first resonance in bending vibration.

For more information regarding the experimental tests, please see the companion paper Vibration-Based Damage Identification Applied for Composite Plate: Experimental Analyses

3.2 Numerical simulations and models

The finite element model, previously presented, was implemented in Abaqus with its UEL (User Element) subroutine and was used to make modal and frequency simulations of the same composite plate studied in the experimental tests. For that, a finite element model of the beam, both undamaged and with the drilled hole was created in Abaqus using the material properties found in the works of Ribeiro et al. (2012). The material properties and geometric dimensions used for the piezoelectric sensors were obtained from the work of Medeiros (2012), which used a micro-structure analysis using FEM and the material and geometrical of fibers and matrix of the piezoelectric sensor to obtain homogenized properties. More details about this methodology for the homogenization of the properties can be found in Medeiros (2012).

The mesh used for the undamaged model as well as the grid used to identify the impact points; accelerances measurements points A1 and A2; and piezoelectric sensors nomenclatures are shown in Fig. 4a. The mesh used for the damaged structure is shown in Fig. 4b. The same impact points and accelerance measurement points were used. It should be noted that these points coincide with some of the actual impact points and points containing accelerometers in the experiment, and are the points chosen for the best results. For the simulation of the experimental boundary conditions two spring elements with a spring coefficient of 1 kN/m were used. Also, an equipotential condition for the electric difference of potential over the piezoelectric sensors was used, as shown by Fig. 5.

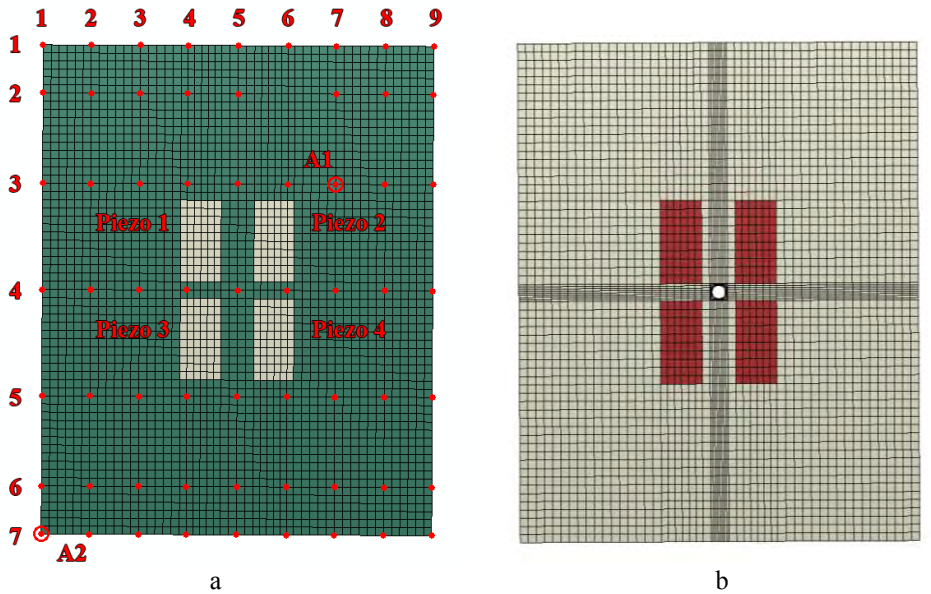

Figure 4. Meshes used in the numerical analysis and points of interest: a) Undamaged structure; b) Damaged structure.

ISSN 2176-5480

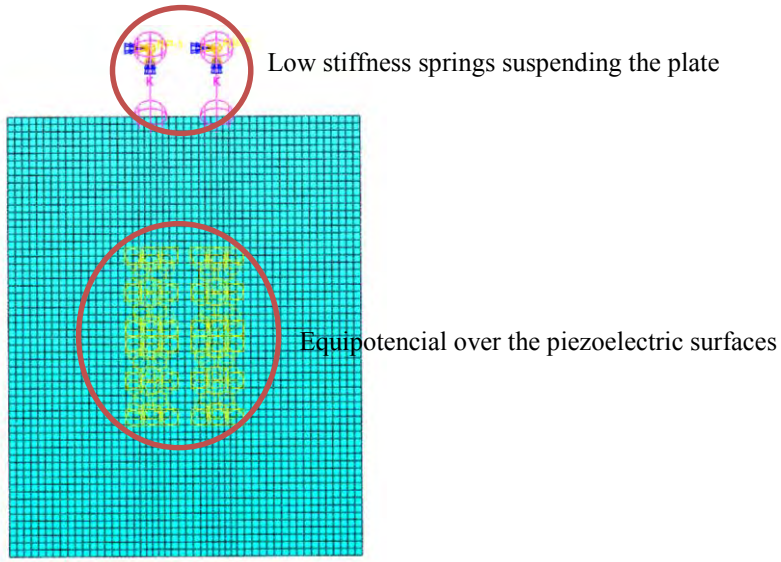

Figure 5. Boundary conditions of the numerical model.

Using the aforementioned material properties and models, undamped frequency domains analyses were made with a concentrated pulse load applied to the same point as in the experimental results. The analysis were chosen as undamped as the structure damping needs to be obtained experimentally. This was make sure the results of each of the methods used, numerical and experimental, were independent from each other.

4. RESULTS AND DISCUSSION

At first, the numerical and experimental results were compared with objective of model validation, identification of its limitations and for a better understanding of the different effects occurring with the experiment. In this step, as for a better comparison between numerical and experimental data, natural frequencies and accelerance frequency response functions from the points with accelerometers in the experiment were compared. After, the damaged and undamaged results for the numerical simulations for the piezoelectric sensors response were compared and its results are discussed.

4.1 Numerical x Experimental Results

At first, the numerical and experimental data were compared. Table 1 shows the first five natural frequencies found experimentally and numerically. It can be noted that the frequencies show a little variations between the FEM model and the experiment, except for the first mode. This probably occurs due to the difficult of first-order shear theory based element in predicting out of the plane torsion modes summed to the boundary conditions used and the inclusion of the piezoelectric sensors, which added an increased mass and stiffness in the model. Also, it should be noted that, as the analysis were undamped, discrepancies between the frequencies should occur, and due to the curvature of the plate, the first torsion mode has one of the greatest damping values of the structure.

Table 1. Natural frequencies found experimentally and numerically.

Frequency		**ω_1 [Hz]**	**ω_2 [Hz]**	**ω_3 [Hz]**	**ω_4 [Hz]**	**ω_5 [Hz]**
Mode Type		1st torsion	1st flexural	2nd torsion	2nd flexural	3rd torsion
Intact	Experimental	61.313	148.847	159.824	222.023	249.610
	Numerical	53.626	150.51	163.16	224.55	252.84
% Difference		14.33%	1.10%	2.04%	1.13%	1.28%
Damaged	Numerical	59.515	149.320	158.055	223.055	249.574
	Experimental	53.598	150.51	163.04	223.80	252.84
% Difference		11.04%	0.79%	3.06%	0.33%	1.29%

The H27.2FRFs for the undamaged and damaged structure is shown in Fig. 7. These specific FRFs were chosen as they were used in deeper experimental analysis and are some of the obtained pair that does not present anti-resonances. As such, the data for each vibration mode can be decoupled and better studied for damage detection purposes.

ISSN 2176-5480

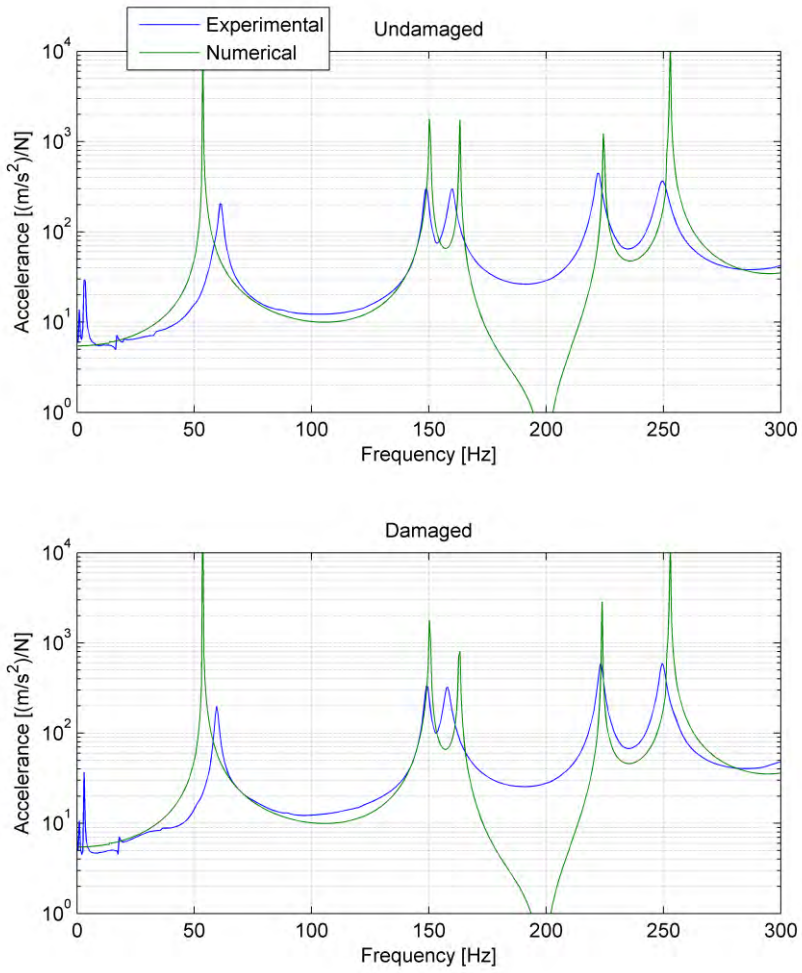

Figure 7. Numerical FRFs for the each piezoelectric sensor for the undamaged and damaged cases.

Some discrepancies between the shape of the frequency response functions found in the experiments and the implemented model can be seem. However, these are explained by both the numerical analysis being undamped and the inclusion of the piezoelectric sensors adding mass and stiffness to the system. Also, the points for both input and output evaluated at the numerical problem are not exactly the same as the ones used in the experiments due to imprecisions in the experimental impact points and accelerometers errors.

4.2 Damaged x Undamaged Comparison and Piezoelectric Sensor Results

The magnitude voltage measured in the piezoelectric sensors per force FRFs are found in Fig. 8. It can be seem that the damage was better perceived in the fourth mode of vibration. That occurs as this is a flexural mode with nodal points in the areas of the sensors, which function based on strains.

ISSN 2176-5480

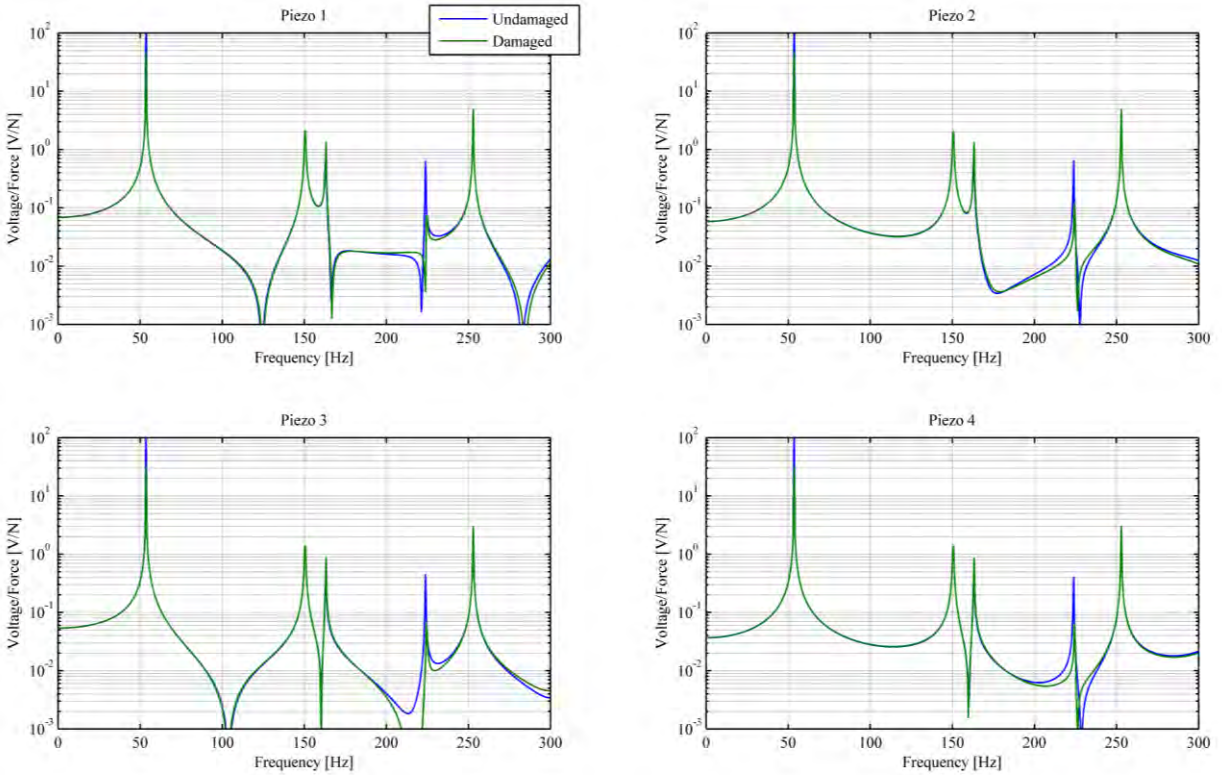

Figure 8. Numerical FRFs for the each piezoelectric sensor for the undamaged and damaged cases.

The difference ratio between the accelerance FRFs for H27.2 and the magnitude for the piezoelectric measures are found in Fig. 9 and 10. It can be observed that the piezoelectric sensors observed the damaged in a broader range of modes. However, both measures observed the damage in the regions of the resonance. Also the values of the ratios are large due to undamped nature of the simulation, which increases the resonance magnitude values

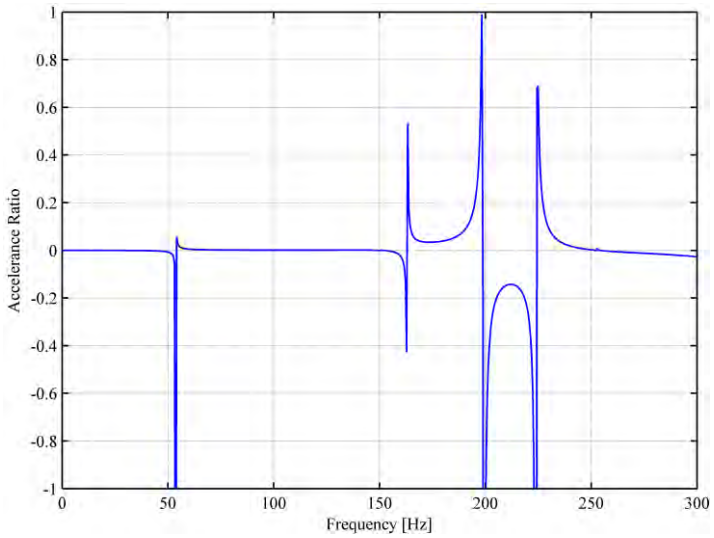

Figure 9. Accelerance difference ratios between the H27.2 FRFs the damaged and undamaged cases.

ISSN 2176-5480

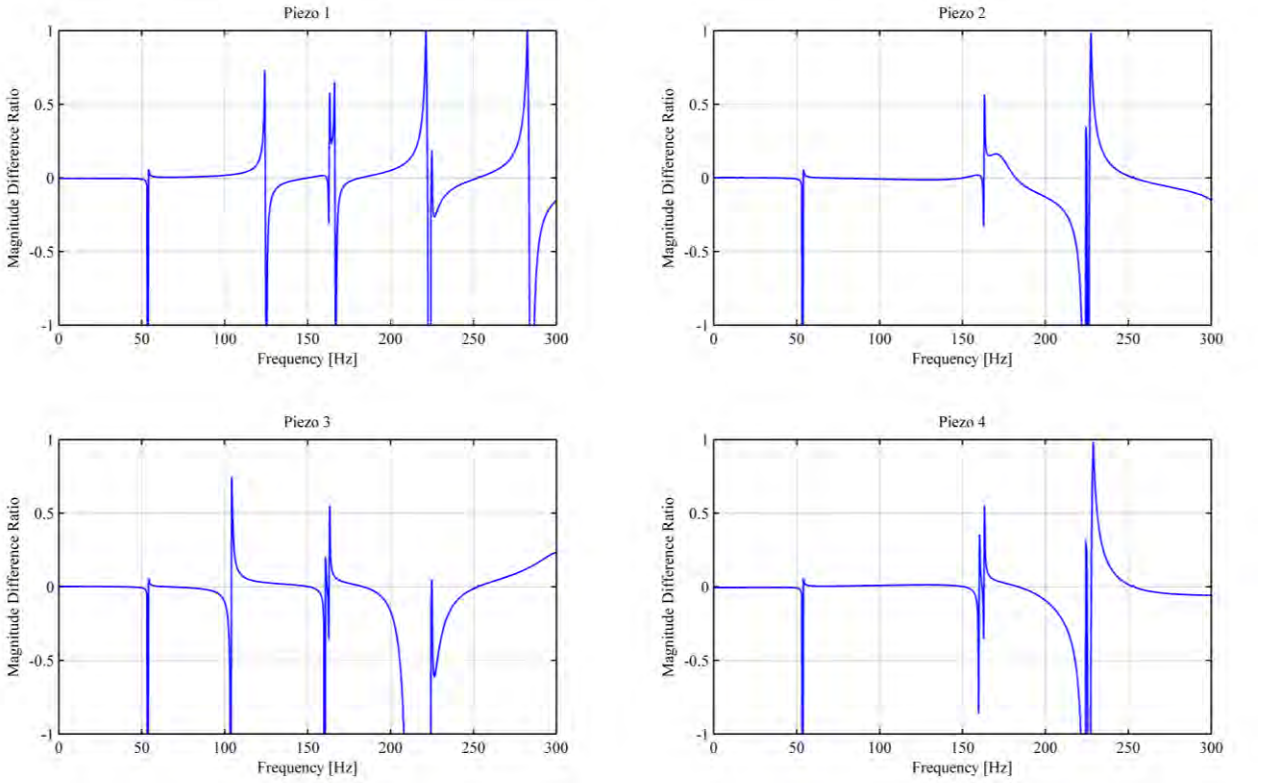

Figure 10. Magnitude difference ratios between the FRFs for the piezoelectric sensors between the damaged and undamaged cases.

5. CONCLUSIONS

In this paper, a carbon-epoxy composite plate containing accelerometers and four piezoelectric patches used as sensors was analyzed experimentally and numerically through finite element analysis using the commercial FEM package Abaqus. For the numerical analysis, a shell finite element containing electro-mechanical coupling effects to account for piezoelectric sensors was implemented in Abaqus using its UEL subroutine. The analyses and experiments were made for both the undamaged structure and a simulated damaged structure, with a hole drilled in its center.

The resonance frequencies found by both the experimental and numerical results for the different level of damage studied did not change in a significant matter, expect for the first vibration mode, due to boundary condition effects. Some discrepancies between the shape of the frequency response functions found in the experiments and the implemented routine were found, but this fact was addressed due to some differences in the experiment and the numerical simulations as boundary conditions and mainly damping effects. Also, the FRFs found by the numerical model were close to the experimental data, proving the effective of the method to calculate the mechanical behavior of smart composites.

The simulations of the piezoelectric sensors proved efficient in showing the potential such transducers have for SHM applications as, for the studied example, the results of direct difference in FRFs for the damaged and undamaged structures were better seem in the piezoelectric signals than in the accelerances.

However, the results found some limitations in using the pure data from the frequency responses of structures as, except for some specific modes and point combinations; a small difference between the damaged and undamaged structures was observed. This fact happened especially in the numerical example as the simple drilling of a small hole in the structure cause a local change in the mass and stiffness of the model that is difficult to detect using global parameter such as FRFs. Not only that, the greatest change in the structure dynamics from damage is a change in damping, that was ignored in the numerical simulations due to those being undamped.

This shows that reeling in pure FRF data is not enough for SHM technics, and more complex metrics based upon modal shapes, resonance peaks, damping, phase or its derivates needs to be used for better prediction of damage. Finally, it is noted that future works will make use of experiments with actual piezoelectric sensors on the structure for better comparison and validation of the finite element model.

ISSN 2176-5480

6. REFERENCES

Carden, E.P. and Fanning, P. (2004). Vibration based condition monitoring: A review. Structural Health Monitoring, Vol. 3, No. 4, pp. 355–377.

Damjanovic, D. (2006). Hysteresis in Piezoelectric and Ferroelectric Materials. In: Bertotti G.; Mayergoyz, I. D. The Science of Hysteresis. Academic Press, Cap. 4, pp. 337-465

Deraemaeker, A.; Nasser, H.; Benjeddou, H.; Preumont, A. (2009). Mixing rules for Macro Fiber Composites (MFC). Journal of Intelligent Material Systems and Structures, vol. 20(12), pp. 1475-1482

Doebling, S.W., Farrar, C.R., Prime, M.B. and Shevitz, D.W. (1996). Damage identification and health monitoring of structural and mechanical systems from changes in their vibration characteristics: A literature review. Technical report, Los Alamos National Laboratory Report LA-13070-MS, Los Alamos, New Mexico.

Fan,W. and Qiao, P. (2011). Vibration-based damage identification methods: A review and comparative study. Structural Health Monitoring, Vol. 10, No. 1, pp. 83–111.

Liu, Y. and Nayak, S. (2012). Structural health monitoring: State of the art and perspectives. Journal of the Minerals, Metals & Materials Society, Vol. 64, No. 7, pp. 789–792.

Marinkovic, D.; Köppe H.; Gabbert, U. (2007). Accurate Modeling of the Electric Field within Piezoelectric Layers for Active Composite Structures. Journal for Intelligent Material Systems and Structures, vol. 18, pp. 503-514.

Medeiros, R. (2012) Desenvolvimento de uma Metodologia Computacional para Determinar Coeficientes Efetivos de Compósitos Inteligentes. USP/EESC. (Dissertação Mestrado).

Montalvão, D., Maia, N. and Ribeiro, A. (2006). A review of vibration-based structural health monitoring with special emphasis on composite materials. Shock and Vibration Digest, Vol. 38, No. 4, pp. 295–324.

Paik, S. H.; Yoon, T. H.; Shin, S. J.; and Kim, S. J. (2007) Computational material characterization of active fiber composite. Journal of Intelligent Material Systems and Structures, Vol. 18, No. 1, Sage Publications, pp.19-28.

Qatu, M. S.; Sullivan, R. W.; Wang, W. (2010). Recent research advances on the dynamic analysis of composite shells: 2000-2009, Composite Structures, vol. 93, pp. 14-31.

Ribeiro, M.L., Tita, V. and Vandepitte, D., 2012. "A new damage model for composite laminates". Composite Structures, Vol. 94, No. 2, pp. 635 – 642.

Salawu, O. (1997). Detection of structural damage through changes in frequency: a review. Engineering Structures, Vol. 19, No. 9, pp. 718 – 723.

Sartorato, M. (2012). Desenvolvimento de um Elemento Finito para Análise de Compósitos Inteligentes: Formulação, Implementação e Avaliação. USP/EESC – São Carlos (Dissertação – Mestrado).

Tita, V., de Carvalho, J. and Vandepitte, D., 2008. "Failure analysis of low velocity impact on thin composite laminates: Experimental and numerical approaches". Composite Structures, Vol. 83, No. 4, pp. 413 – 428.

Wang, J. and Qiao, P. (2007). Improved Damage Detection for Beam-type Structures using a Uniform Load Surface, Structural Health Monitoring, Vol. 6, No. 2, SagePublications, pp.99-110.

Worden, K., Farrar, C.R., Haywood, J. and Todd, M. (2008). A review of nonlinear dynamics applications to structural health monitoring. Structural Control and Health Monitoring, Vol. 15, No. 4, pp. 540–567.

Zienkiewicz, O. C., Taylor, R. L. (2000). The Finite Element Method, Butterworth Heinemann, Second Edition.

Zou, Y., Tong, L. and Steven, G., 2000. "Vibration-based model-dependent damage (delamination) identification and health monitoring for composite structures a review". Journal of Sound and Vibration, Vol. 230, No. 2, pp. 357 – 378.

7. ACKNOWLEDGEMENTS

The authors would like to thank Sao Paulo Research Foundation (FAPESP processes numbers: 2010/13596-0 and 2012/01047-8), as well as National Council for Scientific and Technological Development (CNPq process number: 135652/2009-0), and FAPEMIG for partially funding the present research work through the INCT-EIE.

8. RESPONSIBILITY NOTICE

The authors are the only responsible for the printed material included in this paper.